

Nonequilibrium superconductivity and quasiparticle dynamics in $\text{YBa}_2\text{Cu}_3\text{O}_{7-\delta}$

R. D. Averitt, G. Rodriguez, A. I. Lobad, J. L. W. Siders, S. A. Trugman, and A. J. Taylor

Los Alamos National Laboratory, MS K764, Los Alamos, New Mexico 87545

(Received 24 October 2000; published 12 March 2001)

We have measured, using optical-pump terahertz-probe spectroscopy, the ultrafast (*ab*)-plane conductivity dynamics of quasiparticles and superconducting pairs in $\text{YBa}_2\text{Cu}_3\text{O}_{7-\delta}$ ($\delta=0, 0.5$) thin films from 4 K to T_c . In optimally doped films, the recovery time for long-range phase-coherent pairing increases from ~ 1.5 ps at 4 K to ~ 3.5 ps near T_c , consistent with the closing of the superconducting gap. For underdoped films, the measured recovery time is temperature independent (3.5 ps) in accordance with the presence of a pseudogap. These results are compared to all optical pump-probe measurements at 1.5 eV.

DOI: 10.1103/PhysRevB.63.140502

PACS number(s): 74.72.Bk, 74.40.+k, 78.47.+p, 74.25.Nf

While the precise mechanism for pairing in high- T_c superconductors (HTSC) has yet to be unambiguously determined, the past several years have resulted in significant improvements in our understanding of these fascinating materials. This understanding has been fueled in large part by improvements in the growth of high-quality single crystals coupled with experiments such as neutron scattering and high-resolution angle-resolved photoemission spectroscopy.¹⁻⁴ Ultimately, a more complete understanding of the ground-state properties of HTSC will require further efforts in this direction. However, studies on thin films will continue to play an important role in elucidating the properties of HTSC for several reasons. For a variety of experimental techniques it is difficult or impossible to utilize single crystals. Equally important is the fact that many practical applications of HTSC ranging from gigahertz electronics for satellite communications to broad-band high-sensitivity photon detectors require thin-film structures.⁵ It is also worth emphasizing that such technological applications require a thorough understanding of the excited-state, or nonequilibrium, properties of HTSC which, to date, has not been achieved.

Ultrafast all-optical pump-probe experiments have provided some insight into the ground state and nonequilibrium properties of HTSC.⁶⁻¹⁰ These time-domain experiments have the ability to temporally distinguish dynamics related to superconductivity. This is important given the multiplicity of similar energy scales in HTSC which can be difficult to spectrally resolve in the frequency domain. However, a potential drawback of time-domain optical experiments is that the probe energy, typically 1.5 eV or greater, is much larger than the relevant energy scales in HTSC (typically several $k_b T_c$), such as the *d*-wave superconducting gap or pseudogap. In a few cases, optical pump, far-infrared probe experiments have been used to study HTSC and conventional superconductors.¹¹⁻¹³ For example, 1.6 eV pump, 60–180 meV probe (*ab*)-plane ultrafast reflectivity measurements have been performed on optimally and underdoped YBCO by Kaindl, *et al.*¹³ They measured the ultrafast recovery of both the superconducting condensate and pseudogap correlations whose amplitude showed the same temperature dependence as the 41 meV peak observed in neutron scattering. This suggests that antiferromagnetic fluctuations play a role in pairing in HTSC.

Terahertz time-domain spectroscopy (TTDS) is an ultrafast optical technique in which near single-cycle free-space electric field transients are used to measure the complex conductivity ($\sigma = \sigma_{re} + i\sigma_{im}$) of a material.¹⁴ The electrical pulses contain Fourier components from ~ 100 GHz to several THz (i.e., ~ 0.4 meV–15 meV) making them an ideal source for submillimeter-wave studies of the electrodynamics in superconductors. As representative examples, TTDS has been used to study the vanishing of phase coherence in $\text{Bi}_2\text{Sr}_2\text{CaCu}_2\text{O}_{8+\delta}$ (Ref. 15) and for the observation of the *c*-axis Josephson plasma resonance in $\text{Tl}_2\text{Ba}_2\text{CaCu}_2\text{O}_8$.¹⁶ The THz pulses are derived from femtosecond optical pulses and therefore the optical and THz pulses are temporally coherent. Thus, a sample can be optically excited and then probed with a THz pulse (as a function of the relative arrival time between the optical and THz pulses) to measure induced conductivity changes on an ultrafast timescale.

We have used this experimental technique, known as time-resolved terahertz spectroscopy (TRTS), to measure the conductivity dynamics (both σ_{re} and σ_{im}) in $\text{YBa}_2\text{Cu}_3\text{O}_{7-\delta}$ (YBCO_{7- δ}) for $\delta=0, 0.5$ with picosecond resolution. Importantly, by probing σ , we are able to monitor the dynamics associated with the interplay between the quasiparticle and superconducting pairs. Caution is required in interpreting the dynamics as artifacts are possible. This has been the subject of an earlier publication.¹⁷ In optimally doped films, the recovery time for long-range phase-coherent pairing increases from 1.5 ps at 4 K to ~ 3.5 ps near T_c , consistent with the closing of the superconducting gap. For underdoped films, the measured recovery time is temperature independent (3.5 ps) in accordance with the presence of a pseudogap. These TRTS results differ from all-optical pump-probe measurements at 1.5 eV as discussed in more detail below.

The films used in these experiments were grown on $\langle 100 \rangle$ single crystal MgO substrates using off-axis rf magnetron sputtering resulting in twinned crystalline films with the *c*-axis perpendicular to the plane of the substrate. The $\text{YBa}_2\text{Cu}_3\text{O}_{7-\delta}$ $\delta=0$ (0.5) films were 50 (300) nm thick. T_c was 85 K (50 K) for the $\delta=0$ (0.5) films. The experiments utilized a commercial-based regeneratively amplified Ti:Al₂O₃ system operating at 1 KHz and producing nominally 1.0 mJ, 150 fs pulses at 1.5 eV. The THz pulses were generated and detected using electro-optic techniques. A He

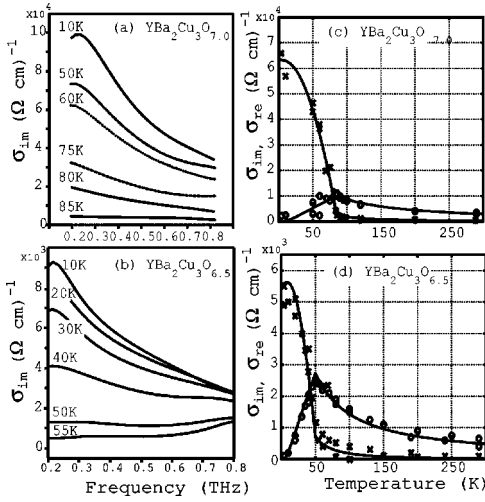


FIG. 1. (a) and (b) σ_{im} as a function of frequency for the $\delta = 0$ and 0.5 films, respectively. (c) and (d) show the temperature dependence of σ_{re} (O) and σ_{im} (X) at 500 GHz. The solid lines are fits using Eq. (1).

cryostat permitted temperature-dependent measurements from 4–300 K. Further details of the TRTS experiments are described elsewhere.¹⁷

Figures 1(a) and 1(b) shows the imaginary conductivity from 0.2 to 0.8 THz at various temperatures for the $\delta = 0$ and 0.5 films, respectively. Below T_c , σ_{im} displays a clear $1/\omega$ dependence. The real part of the conductivity (not shown) is relatively flat over this frequency range. These results are similar to other THz experiments on YBCO thin films.^{18–21} For the present discussion, the two-fluid model, which has been extensively used in describing the complex conductivity in superconductors will be employed.¹⁹ In this model, the conductivity is composed of two components: an imaginary component that is dominated, below T_c , by the superfluid population and a Drude component that is proportional to the fraction of quasiparticles in the normal state. The complex conductivity is given by

$$\sigma(\omega, T) = \sigma_{re} + i\sigma_{im}$$

$$= \frac{ne^2}{m^*} \left\{ \frac{f_n(T)}{\tau(\omega, T)^{-1} - i\omega} + f_s(T) \left[\frac{i}{\omega} + \pi\delta(\omega) \right] \right\}, \quad (1)$$

where the first term corresponds to the normal fraction and the second term to the superconducting fraction. In this equation, n is the total carrier concentration, m^* is the effective mass, $f_n(T)$ and $f_s(T)$ are the normal and superconducting fractions ($f_n + f_s = 1$), respectively, $\tau(\omega, T)$ is the carrier collision time for the normal fraction, and T is the temperature. The temperature dependence of the conductivity arises from the temperature dependence of f_n , f_s , and τ .

Figures 1(c) and 1(d) shows the measured complex conductivity versus temperature at 500 GHz for $\delta = 0$ and 0.5 films. The crosses and circles are the experimentally measured values for the imaginary and real parts of the conductivity, respectively. These results, in agreement with other

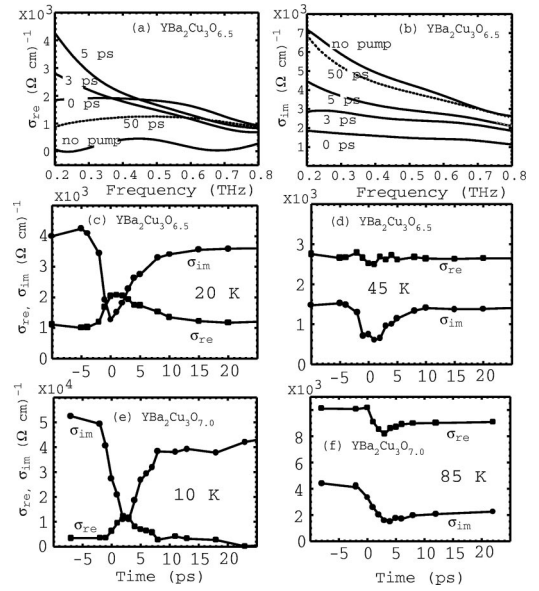


FIG. 2. (a) and (b) σ_{re} and σ_{im} versus frequency at various delay times subsequent to optical excitation for $\delta = 0.5$. (c) and (d) The temporal dependence of the conductivity (0.5 THz) at initial temperatures of 20 and 45 K for YBCO_{6.5}. (e) and (f) The temporal dependence of the conductivity (0.5 THz) at initial temperatures of 4 and 85 K for YBCO_{7.0}. The lines in (c)–(f) are to guide the eye.

studies, show that as the temperature is decreased below T_c , there is a dramatic increase in σ_{im} related to an increase in the superfluid population. In comparison, σ_{re} first increases with decreasing temperature above T_c and then decreases below T_c . This peak in the temperature dependence of σ_{re} is due to an increase in τ with decreasing temperature which is eventually offset by a decrease in f_n below T_c . The solid lines in Fig. 1(c) are calculations using the two-fluid model [Eq. (1)] with $f_s = 1 - (T/T_c)^2$, which is what is expected for d-wave pairing with strong impurity scattering.²² This model fits the experimental data reasonably well and aids in understanding the dynamics measurements. Most importantly, σ_{im} is a measure of the superconducting fraction, and σ_{re} is a measure of the quasiparticle fraction and scattering time. Thus, upon optical excitation, the picosecond dynamics of each component can be determined.

Photoexcitation of YBCO in the superconducting state with a 150 fs, 1.5 eV pulse breaks superconducting pairs resulting in a decrease of f_s and a commensurate increase of the quasiparticle fraction, f_n . Below T_c , a transient decrease in σ_{im} and an increase in σ_{re} is expected [see Eq. (1) or Figs. 1(c) and 1(d)]. It is important to note that in making these measurements the conductivity has to be measured at each delay between the optical and THz pulses. This is because optical excitation modifies both σ_{re} and σ_{im} meaning that both the amplitude and phase of the THz electric field change. Therefore it is not sufficient to sit at the peak of the electric field and scan the optical delay line to measure the dynamics. Figures 2(a) and 2(b) show the transient changes in the real and imaginary conductivity for a $\delta = 0.5$ sample at 10 K after excitation with a 150 fs 60 μ J optical pulse corresponding to an initially photoexcited quasiparticle density

of $\sim 4 \times 10^{19} \text{ cm}^{-3}$. There is a sharp decrease in σ_{im} and an increase in σ_{re} . Similar behavior is observed for the optimally doped films. Figures 2(c) and 2(d) show σ_{re} and σ_{im} at 500 GHz as a function of time at 20 and 45 K, respectively, for YBCO_{6.5}. Figures 2(e) and 2(f) show similar plots for the YBCO_{7.0} film at 4 and 85 K. These data clearly show that upon optical excitation, there is a strong decrease in the superconducting carrier fraction which partially recovers on a picosecond time scale. The incomplete conductivity recovery at longer times arises from the creation of a large number of phonons in the film as the quasiparticles relax. On a ns time scale the film returns to the initial temperature (and conductivity) as the phonons leave the film via thermal transport to the substrate.

To determine the superconducting pair recovery time τ_σ in a consistent manner we fit the decay of the integrated square of the electric field as a function of pump-probe delay to an exponential curve with decay time τ_σ plus an offset. We have included the width of the THz probe pulse by performing a convolution between a 2.5 ps Gaussian pulse with the exponential decay. The temporal evolution of the electric field squared (normalized to 1) is shown in Fig. 3 at various temperatures for the (a) YBCO_{7.0} and (b) YBCO_{6.5} films. The circles are the data and the lines are the best fits (τ_σ) and fits using $\tau_\sigma \pm 0.5$ ps. Reasonable exponential fits are obtained at all temperatures. The lifetime τ_σ determined at each temperature using this procedure is shown in Fig. 3(c). The error bars are one standard deviation in magnitude. For optimal doping (circles), τ_σ increases from ~ 1.5 ps at 4 K to ~ 3.5 ps near T_c . Thus it appears that the increase in lifetime follows the closing of the superconducting gap $\Delta(T)$. This temperature dependence [i.e., $\tau_\sigma \propto 1/\Delta(T)$] has been predicted theoretically and observed in aluminum where the timescales are much longer.^{23,24} In contrast to the optimally doped films, the lifetime for the $\delta=0.5$ film (triangles) is approximately 3.5 ps and is independent of temperature—i.e., τ_σ does not follow $1/\Delta(T)$. The dynamics in this case appear to be influenced by the pseudogap which is thought to be a gap that arises in the density of states due to quasiparticle pairing without the requisite long-range phase coherence necessary for superconductivity. The conductivity dynamics cannot be measured up to $k_b T^*$ (the pseudogap energy) because the induced changes in σ are too small to measure at temperatures significantly above T_c . However, we have observed a resolution limited response above T_c for the optimally doped films that is probably due to electron-phonon equilibration.

These experiments, due to signal-to-noise considerations, have been performed at a relatively high fluence (50–100 $\mu\text{J}/\text{cm}^2$). That is, the superconductivity is strongly perturbed in that the condition $\Delta\sigma/\sigma \ll 1$ is not satisfied. For example, in Fig. 2(c) σ_{im} decreases by $\sim 30\%$. For the YBCO_{7.0} film at 4 K, the film is almost driven normal upon optical excitation [Fig. 2(e)]. Therefore f_n increases significantly from ~ 0 with a correspondingly large decrease in f_s . In addition to these changes in carrier fractions, the superconducting order parameter is strongly modified since it is temperature depen-

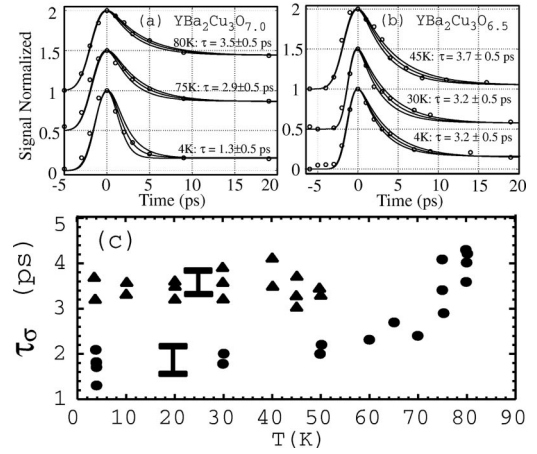


FIG. 3. (a) and (b) Temporal evolution of the electric field squared and normalized at various temperatures for YBCO_{7.0} and YBCO_{6.5}, respectively. The circles are the data and the lines fits as described in the text. The curves are vertically displaced for clarity. (c) Measured lifetime, τ_σ , as a function of temperature. The circles are for $\delta=0.0$, and the triangles are for $\delta=0.5$.

dent. Despite the strong optical perturbation, the changes in τ_σ for the YBCO_{7.0} and YBCO_{6.5} films are distinctly different as Fig. 3 demonstrates.

The observed dynamics cannot be fully explained in terms of nonequilibrium theory developed for conventional superconductors.^{25,26} There are primarily two reasons for this. First, the d -wave symmetry needs to be considered. Kabanov *et al.* have interpreted all-optical pump-probe measurements as arising from the anharmonic decay of phonons with energies greater than 2Δ .⁹ Quasiparticles continue to be generated from superconducting pairs as long as phonon modes with energy $>2\Delta$ are populated (and thus available for superconducting pair annihilation.) Using Eq. (25) from Kabanov *et al.* and data for the A_{1g} apical oxygen phonon mode in YBCO, we estimate $\tau_\sigma = 1.6$ ps at 60 K which is in reasonable agreement with the measured value of ~ 1.5 ps for the YBCO_{7.0} film. Furthermore, Kabanov *et al.* predict $\tau_\sigma \propto 1/\Delta$ meaning that, upon approaching T_c , τ_σ should increase as they have observed in all-optical measurements and as we have observed in our TRTS experiments. However, the temperature dependence they present assumes an s -wave dependence for the order parameter. This is clearly at odds with the established d -wave symmetry of the order parameter in the cuprates. The nodes in the d -wave gap along $k_x = k_y$ in the Brillouin zone could strongly modify the phonon bottleneck as posited in models which treat a fully gapped superconductor. Alternatively, and supported by the experiments to date, if the quasiparticle relaxation occurs away from $k_x = k_y$, a situation similar to a fully gapped superconductor is possible.

Secondly, the role of pseudogap correlations in determining the complex conductivity requires further investigation. The two-fluid model described above is incapable of explaining the effect of pseudogap correlations in determining $\sigma(\omega)$. It is possible that the observed temperature dependence of the dynamics for the underdoped film results from sitting at the low-energy edge of the pseudogap similar to

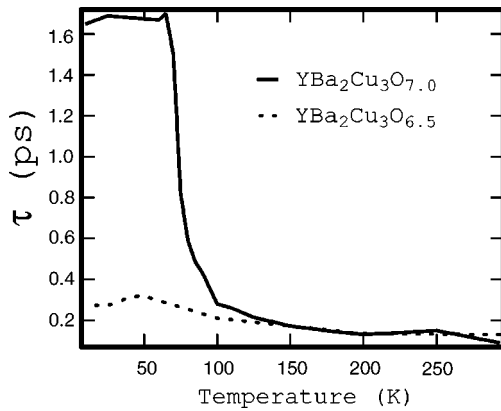


FIG. 4. Measured lifetimes as a function of temperature using all optical pump-probe spectroscopy. The solid line is for YBCO_{7.0} and the dotted line is for YBCO_{6.5}.

what has been observed at higher probe energies by Kaindl *et al.*¹³ In order to further clarify the nonequilibrium dynamics in the cuprates, experiments need to be performed on the same films, at fixed excitation fluence and at various probe wavelengths from ~ 1 meV to 1 eV.

Along these lines, we have performed all-optical pump probe experiments at 1.5 eV on our YBCO_{7.0} and YBCO_{6.5} thin films. Our results are in agreement with other all-optical pump-probe measurements.^{6–10} The measured lifetimes as determined from the induced change in transmission at 1.5 eV, are shown as a function of temperature in Fig. 4. The solid line is for YBCO_{7.0} and the dotted line is for YBCO_{6.5}. For the optimally doped film the lifetime below T_c is about 1.7 ps in good agreement with our TRTS measurements.

Above T_c , the lifetime drops to a few hundred fs—this is just a measure of the electron phonon relaxation time.⁷ Interestingly, for the all-optical experiments, we do not observe an increase in the lifetime upon approaching T_c from below yet the increase is clearly observable in our TRTS measurements [Fig. 3]. For the underdoped film (Fig. 4, dashed line) the measured lifetime decreases slightly from 300 fs at 10 K to about 150 fs at room temperature. This lifetime is an order of magnitude faster than for our TRTS measurements and shows no marked change at any temperature from 10–300 K. This leads us to conclude that it is not clear that all-optical measurements at 1.5 eV on underdoped films probe the dynamics of the pseudogap. It is possible that short-range incoherent pairing fluctuations are being probed. Or, the observed lifetime may just be a measure of the electron-phonon relaxation. This is supported by the similarity of the lifetimes for the underdoped and optimally doped films above T_c as shown in Fig. 4.

In summary, we have measured the ultrafast conductivity dynamics in optimally doped and underdoped YBCO thin films. Our results are consistent with the dynamics being influenced by the superconducting gap, and in the case of the underdoped films, the pseudogap as well. Further development in the theory of nonequilibrium superconductivity in the cuprates is required in order to more fully understand our experimental results.

We would like to thank B. Houlton and F. Garzon for preparing the YBCO films used in these experiments. This research was supported through the Los Alamos Directed Research and Development Program by the U.S. Department of Energy.

¹P. Dai *et al.*, *Science* **284**, 1344 (1999).

²T. Valla *et al.*, *Science* **285**, 2110 (1999).

³J. Orenstein and A. J. Millis, *Science* **288**, 468 (2000).

⁴D. L. Feng *et al.*, *Science* **289**, 277 (2000).

⁵A. R. Jha, *Superconductor Technology* (John Wiley and Sons, New York, 1998).

⁶S. G. Han *et al.*, *Phys. Rev. Lett.* **65**, 2708 (1990).

⁷S. V. Chekalin *et al.*, *Phys. Rev. Lett.* **67**, 3860 (1991).

⁸C. J. Stevens *et al.*, *Phys. Rev. Lett.* **78**, 2212 (1997).

⁹V. V. Kabanov *et al.*, *Phys. Rev. B* **59**, 1497 (1999).

¹⁰J. Demsar *et al.*, *Phys. Rev. Lett.* **82**, 4918 (1999).

¹¹J. F. Federici *et al.*, *Phys. Rev. B* **46**, 11 153 (1992).

¹²G. L. Carr *et al.*, *Phys. Rev. Lett.* **85**, 3001 (2000).

¹³R. A. Kaindl *et al.*, *Science* **287**, 470 (2000).

¹⁴M. C. Nuss and J. Orenstein, in *Millimeter and Submillimeter*

Wave Spectroscopy of Solids, edited by G. Grüner (Springer-Verlag, Germany, 1998).

¹⁵J. Corson *et al.*, *Nature (London)* **398**, 221 (1999).

¹⁶V. K. Thorsmølle *et al.*, in *Ultrafast Phenomena XII*, edited by T. Elsaesser *et al.* (Springer, Berlin, 2001), pp. 431–433.

¹⁷R. D. Averitt *et al.*, *J. Opt. Soc. Am. B* **17**, 327 (2000).

¹⁸M. C. Nuss *et al.*, *Phys. Rev. Lett.* **66**, 3305 (1991).

¹⁹S. D. Brorson *et al.*, *J. Opt. Soc. Am. B* **13**, 1979 (1996).

²⁰I. Francois *et al.*, *Phys. Rev. B* **53**, 12 502 (1996).

²¹A. Pimenov *et al.*, *Phys. Rev. B* **59**, 4390 (1999).

²²A. Hosseini *et al.*, *Phys. Rev. B* **60**, 1349 (1999).

²³M. Tinkham, *Phys. Rev. B* **6**, 1747 (1972).

²⁴I. Schuller and K. E. Gray, *Phys. Rev. Lett.* **36**, 429 (1976).

²⁵A. Rothwarf and B. N. Taylor, *Phys. Rev. Lett.* **19**, 27 (1967).

²⁶S. B. Kaplan *et al.*, *Phys. Rev. B* **14**, 4854 (1976).